A.A. Azami[1],
P. Payvandy[1,*],
M.M. Jalili[2]

Analytical Approach for Simulating the Compression and Recovery Behaviour of Nonwoven Fabrics for Automotive Floor--Covering Application under Static Loading

DOI: 10.5604/01.3001.0014.6503

[1] **Yazd University, Department of Textile Engineering,**
Yazd, Iran,
* e-mail: peivandi@yazd.ac.ir

[2] **Yazd University, Department of Mechanical Engineering,**
Yazd, Iran

Abstract
In this study, viscoelastic model parameters are obtained to predict the compression and recovery behaviour of needle-punched nonwoven textiles which are customarily used in industrial applications such as automotive floor-coverings. To this end, two different models are used to explain the compression and recovery behaviour of non-woven textiles under brief, moderate static loading (BMSL) and prolonged, heavy static loading (PHSL) according to ISO 3415 and ISO 3416, respectively. The first model consists of a linear spring and damper set parallel to each other. This combination is placed in series with a linear damper. The second model, however, consists of a linear spring and damper set parallel to each other and placed in series with a nonlinear damper. The results obtained for the compression and recovery behaviour of the non-woven textiles under BMSL and PHSL are compared with experimental results. The results obtained indicated that the nonlinear model is more accurate in the prediction of the compression and recovery behaviour of needle-punched nonwoven textiles under static loading than the linear model. The best result for the prediction of the compression and the recovery behaviour of nonwoven textiles under BMSL and PHSL occurs with the nonlinear model, in which the errors are 4.68% and 4.66%, respectively, when compared to the experimental results.

Key words: *compression, recovery, nonwoven textile, non-linear Jeffrey's II model, static loading.*

Introduction

Nonwoven textiles have various applications in the industry, such as making household goods, automotive floor-coverings [1], filters and geotextiles. These textiles are subjected to different kinds of force and deformation. One of the important deformations is compression and recovery after the load removal. It has been shown that thickness loss in nonwoven textiles is highly affected by the compression behaviour of the textiles. In recent years, many researchers have taken an interest in the study of the compression and recovery of nonwoven textiles. Khotari and Das [2] studied the time-dependent compression of different nonwoven fabrics. As they observed, recovery from a deformed state increases with an increase in the relaxation time after the compression–recovery cycle. However, the time-dependent effect is insignificant in the case of heat-sealed nonwovens as much of the recovery is instantaneous. In another study, Khotari and Das [3] presented a theoretical analysis of the compressional behaviour of nonwoven fabrics based on their bending properties. They found that spun-bond heat-sealed fabrics are more compatible with the theoretical model as compared to spun-bond needle-punched fabrics. Debnath and Madhusoothanan [4] modelled the compression properties of needle-punched nonwoven fabrics produced from polyester and a blend of jute-polypropylene fibres of varying fabric weight, needle density and blend ratio of jute and polypropylene fibres. The initial thickness, compression percentage, percentage of thickness loss, and compression resilience were predicted using an artificial neural network. Debnath and Madhusoothanan [5] investigated the effects of fabric weight, fibre cross-sectional shapes, and reinforcing materials on the compression properties of polyester needle-punched industrial nonwoven fabrics. They showed that in fabrics with no reinforcing materials, the compression and thickness loss are higher than those in fabrics with reinforcing materials, regardless of fibre cross-sections. They also showed that polyester fabrics made from hollow cross-sectioned fibres have the least rate of compression at every level of fabric weight. In another research, Debnath, and Madhusoothanan [6] investigated the effects of fabric weight, fibre cross-sectional shapes, and reinforcing materials on compression properties under dry and wet conditions of polyester needle-punched industrial nonwoven fabrics. The results showed that compression resilience is higher in round cross-sectional fabrics without reinforcing materials under wet conditions than in fabrics with reinforcing materials. It also emerged that when the fabric weight increases, the initial thickness increases, but the percentage of compression and thickness loss decreases. This is regardless of the fibre cross-sectional shape in either dry or wet conditions. In a subsequent study, Debnath and Madhusoothanan [7] examined the effects of parallel-laid and cross-laid webs of polypropylene needle-punched nonwoven fabrics on their compression properties under wet conditions. Their results showed that an increase in the needle density would lead to a reduction in the initial thickness, compression percentage, and thickness percentage under wet conditions, compared to dry conditions in both parallel-laid and cross-laid fabrics. It was also found that the compression resilience would rise with an increase in the needle density under dry and wet conditions of parallel-laid webs. A linear viscoelastic model was presented by Jafari and Ghane [8] to evaluate the recovery behaviour of machine-made carpets after a brief and heavy static loading (BHSL). Different combinations of spring and damper systems were taken into consideration to model the mechanical behaviour of the carpets. According to the results, there was reasonably good agreement between the Jeffrey's model and experimental findings. It was also revealed that the linear standard model has poor regression for the recovery properties of cut pile carpets after static loading. Khavari and Ghane [9] used three different models to investigate the compression, decompression and recovery of cut pile carpets under BHSL and with a constant rate of compression. The Maxwell mechanical model as well as linear and nonlinear three-element models were used to simulate the compression and recovery behaviour of the carpet samples. The results showed that a three-element model consisting of a Maxwell body paralleled with a non-linear spring can describe compression and decompression more accurately than Maxwell and linear models. Tower and Carrillo [10] predicted the compression behaviour of nonwoven carpets by considering their fibre properties and doing discrete fibre finite element simulation through the Abaqus technique. Jafari and Ghane [11] studied the effect of UV radiation on the recovery behaviour of pile carpets after BHSL through analytical and viscoelastic modelling. The thickness loss and maximum compression both proved to be higher within longer UV exposure times. In their subsequent study in 2018 [12], Jafari and Ghane used the linear and nonlinear Jeffrey's models, as two different mechanical models, to investigate the recovery property of machine-made carpets. It was indicated that, in comparison to the linear model, the nonlinear Jeffrey's model has a lower speed of recovery at zero time.

Although various models are presented to simulate the compression and recovery behaviour of nonwoven textiles, there is little research regarding compression and recovery properties under BMSL and PHSL simultaneously. Also, those researches used curve fitting methods to adapt the experimental data to the theoretical models. Therefore, the purpose of this study is to obtain viscoelastic model parameters analytically to predict the compression and recovery properties of needle-punched non-woven textiles under BMSL and PHSL according to ISO3415 and ISO3416 simultaneously.

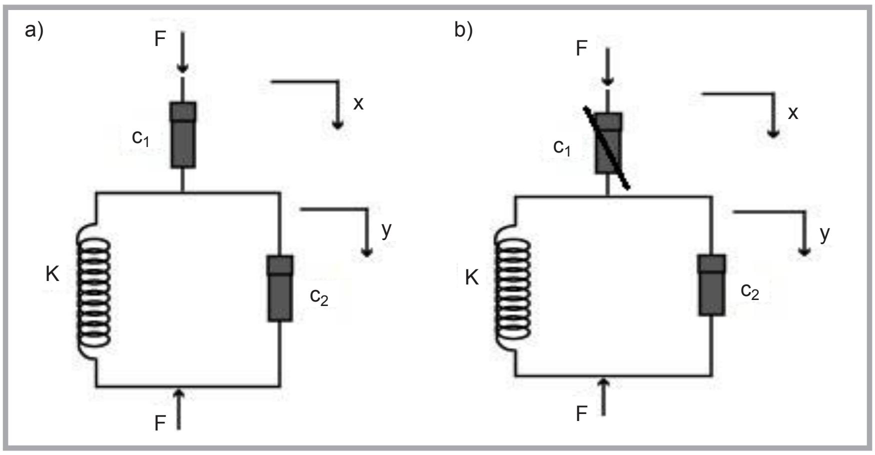

Figure 1. *Mechanical model: a) Linear Jeffrey's model and b) Non-linear Jeffrey's model.*

Mechanical model

To investigate the compression and recovery behaviour of nonwoven fabrics under BMSL and PHSL, two different mechanical models based on mass-spring- dashpot are presented: a) a linear model consisting of a Voigt-Kelvin body that is placed in series with a linear damper and b) a nonlinear model consisting of a Voigt-Kelvin body that is placed in series with a nonlinear damper. It is known as Jeffrey's II model.

Schematic diagrams of the two models are presented in ***Figure 1***.

The compressive force F is applied to every model. As shown in ***Figure 1***, k is the linear spring constant (N/m), and c_1 and c_2 are the damper constants (N·s/m). In the first model, c_1 is a linear damper, while in the second method, c_1 (N·s/m^2) is a nonlinear damper. The governing differential equations for the linear and nonlinear models are presented in the following section.

Linear Jeffrey's II model

Compression

In the Linear Jeffrey's II model, the forces in the dashpot c_1 and in the Voigt-kelvin element are the same. Thus, the compressive force is obtained using ***Equations (1)*** and ***(2)*** [13];

$$F = ky + c_2\dot{y} \tag{1}$$

$$F = c_1(\dot{x} - \dot{y}) \tag{2}$$

Equation (3) can be obtained from ***Equations (1)*** and ***(2)*** as:

$$\dot{F}\left(1 + \frac{c_2}{c_1}\right) + \frac{kF}{c_1} - (k\dot{x} + c_2\ddot{x}) = 0 \tag{3}$$

Because the force F is constant, its derivative is zero, and ***Equation (3)*** can be expressed as follows:

$$c_2\ddot{x} + k\dot{x} = \frac{kF}{c_1} \tag{4}$$

Considering $\dot{x} = u$, ***Equation (4)*** can be written as:

$$\dot{u} + \frac{k}{c_2}u = \frac{kF}{c_1 c_2} \tag{5}$$

Solving the differential ***Equation (5)***, parameter u can be obtained as follows:

$$u = Ae^{\frac{-kt}{c_2}} + \frac{F}{c_1} \tag{6}$$

Where, A is a constant coefficient.

Parameter x can be obtained by integrating from ***Equation (6)***:

$$x = -\frac{Ac_2 e^{\frac{-kt}{c_2}}}{k} + \frac{F}{c_1}t + B \tag{7}$$

Where, B is a constant coefficient.

Determining the response of the system from ***Equation (7)*** needs two initial conditions. Introducing the initial conditions $t = 0$, $x = 0$ and $u = 0$ into ***Equations (6)*** and ***(7)***, constants A and B can be obtained as follows:

$$A = -\frac{F}{c_1} \tag{8}$$

$$B = \frac{Ac_2}{k} \tag{9}$$

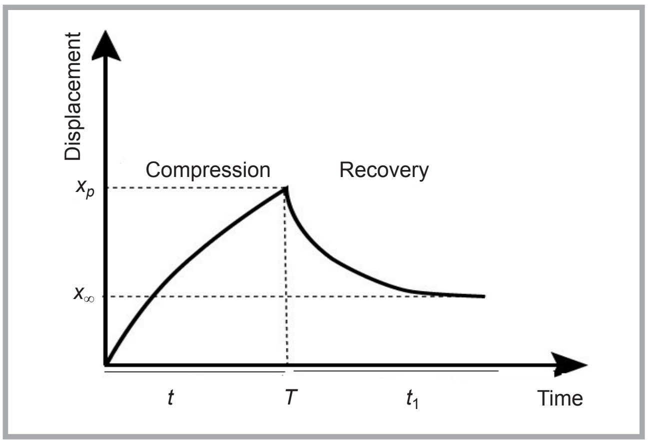

Figure 2. *Compression and recovery behaviour of nonwoven textiles during loading and after its removal.*

Recovery

Since the start point in the recovery is equivalent to the end point of the compression, the initial conditions for this case are:

$$x(t_1) = x^* \tag{10}$$

$$u(t_1) = R_r \tag{11}$$

Where, t_1 is the recovery time.

After the constant load applied is removed, the recovery (or stress relaxation) equations can be calculated. Considering $F = 0$ and substituting it into ***Equation (7)***, ***Equation (12)*** can be achieved, in which the constant parameters and time are changed in ***Equation (7)***.

$$x^* = x(t_1) = -\frac{\hat{A}c_2 e^{\frac{-kt_1}{c_2}}}{k} + \hat{B} \tag{12}$$

$$R_r = u(t_1) = \hat{A}e^{\frac{-kt_1}{c_2}} \tag{13}$$

Where, R_r is the slope of the recovery diagram at the first point.

As shown in ***Figure 2***, x_p is the maximum compression, and x_∞ is the last displacement in the recovery section. Now, x_p and x_∞ are substituted into ***Equation (12)***:

$$\frac{-\hat{A}c_2}{k} e^{\frac{-kt_1}{c_2}} = x_p - x_\infty \tag{14}$$

Since $x_\infty = \hat{B}$, hence:

$$\frac{R_r c_2}{k} = x_\infty - x_p \tag{15}$$

Equation (14) can be rewritten as follows:

$$\frac{c_2}{k} = \frac{x_\infty - x_p}{R_r} = c_2 k \tag{16}$$

The recovery behaviour under BMSL and PHSL is taken into consideration an hour and 24 hours after load removal on the samples, respectively. Also, the displacement at the start point of unloading is equal to the end point of loading ($x_p = x^*$). Therefore, the initial point of recovery can be calculated as:

$$x_p = -\frac{Ac_2 e^{\frac{-kT}{c_2}}}{k} + \frac{F}{c_1}T + B = \\ = -\hat{A}\frac{c_2}{k}e^{\frac{-kT}{c_2}} + \hat{B} \tag{17}$$

$$\hat{B} = \frac{c_2 e^{\frac{-kT}{c_2}}}{k}\left(\hat{A} - A\right) + \frac{F}{c_1}T + B \tag{18}$$

In order to calculate the constant coefficients $(A, B, \hat{A}, \hat{B})$ and model parameters (k, c_1, c_2), ***Equation (12)*** is solved analytically, and parameters and are calculated as follows:

$$x = -\frac{Ac_2 e^{\frac{-kT}{c_2}}}{k} + \frac{F}{c_1}T + B \tag{19}$$

$$u = Ae^{\frac{-kt_1}{c_2}} + \frac{F}{c_1} \tag{20}$$

In $T = 7200$, $x = x_p$ and the slope of the initial position in the compression diagram is equal to the slope of the experimental diagram. If it is assumed that the diagram of thickness variation against time is linear and the value of $Ae^{\frac{-kt_1}{c_2}}$ is ignorable, then:

$$\frac{F}{c_1} = \frac{x_p}{T} \tag{21}$$

Equation (22) is derived from the first derivation of ***Equation (12)*** as follows:

$$\dot{u} = \hat{A}e^{\frac{-kt_1}{c_2}} \tag{22}$$

In $T = 7200$ s, the slope is equal to that of the loading diagram at the first point (R_r), which is defined as:

$$R_r = \hat{A}e^{\frac{-kT}{c_2}} \tag{23}$$

Considering ***Equation (15)***, ***Equation (23)*** can be rewritten as:

$$\frac{c_2}{k} = \frac{x_p - x_\infty}{-R_r} = c_2 k \tag{24}$$

Constants $\hat{A}$ & $\hat{B}$ and x_p can be obtained as follows:

$$\hat{A} = R_r e^{\frac{-kT}{c_2}} \tag{25}$$

$$x_p = \frac{-Ac_2 e^{\frac{-kT}{c_2}}}{k} + \frac{F}{c_1}T + B = \\ = -\hat{A}\frac{c_2}{k}e^{\frac{-kT}{c_2}} + \hat{B} \tag{26}$$

$$\hat{B} = \frac{c_2 e^{\frac{-kT}{c_2}}}{k}\left(\hat{A} - A\right) + \frac{F}{c_1}T + B \tag{27}$$

Non-linear Jeffrey's II model

In the non-linear Jeffrey's II model, damper c_1 is considered to be nonlinear, as presented in ***Equation (28)***:

$$F = c_1(\dot{x} - \dot{y})(x - y) \tag{28}$$

According to ***Figure 1***, the governing differential equation for the linear part of the model under a compressive force is as follows:

$$F = ky + c_2\dot{y} \tag{29}$$

Equation (30) can be calculated by integrating ***Equation (29)*** as:

$$x = -\sqrt{\frac{2(F.t - A)}{c_1}} + y \tag{30}$$

y can be determined from the ordinary differential ***Equation (29)*** as:

$$y = Be^{-\frac{k}{c_2}t} + \frac{F}{k} \tag{31}$$

Equation (32) can be obtained by substituting ***Equation (30)*** into ***Equation (31)*** as follows:

$$x = Be^{-\frac{k}{c_2}t} + \frac{F}{k} - \sqrt{\frac{2(F.t - A)}{c_1}} \tag{32}$$

Equation (33) is derived from the first derivation of ***Equation (32)*** as follows:

$$u = \dot{x} = -\frac{k}{c_2}Be^{-\frac{k}{c_2}t} - \frac{F}{c_1}\sqrt{\frac{2(F.t - A)}{c_1}} \tag{33}$$

Introducing the initial conditions $x = 0$, $t = 0$, and $\dot{x} = R_{c0}$, ***Equations (34)*** and ***(35)*** can be obtained as:

$$B - (-\frac{2A}{c_1})^{0.5} + \frac{F}{k} = 0 \tag{34}$$

Figure 3. *Static loading device.*

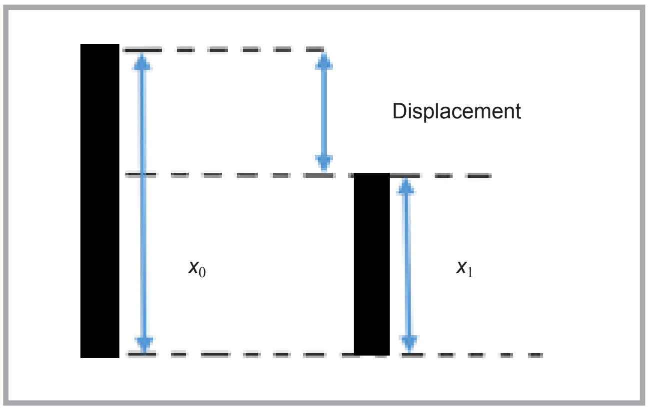

Figure 4. *Schematic diagram of thickness measurement.*

$$-\frac{k}{c_2}B - \frac{F}{c_1}\left(-\frac{2A}{c_1}\right)^{-0.5} = R_{c0} \quad (35)$$

Equation (36) can be calculated from ***Equations (34)*** and ***(35)*** as follows:

$$-\frac{k}{c_2}\left(-\frac{2A}{c_1}\right)^{0.5} - \frac{F}{c_1}\left(-\frac{2A}{c_1}\right)^{-0.5} + \frac{F}{c_2} = R_{c0} \quad (36)$$

For simplification, parameters a and X are introduced as follows:

$$a = -\frac{2A}{c_1} \quad (37)$$

$$X = a^{0.5} \quad (38)$$

Parameter X can be calculated by solving ***Equation (36)*** as follows:

$$X = \frac{(\frac{F}{c_2} - R_{c0}) + \sqrt{\left(\frac{F}{c_2} - R_{c0}\right)^2 - \frac{4k}{c_1}\frac{F}{c_2}}}{2\frac{k}{c_2}} \quad (39)$$

Considering that there is no recovery force, ***Equations (32)*** and ***(33)*** can be rewritten as:

$$x = \hat{B}e^{-\frac{k}{c_2}t} + \left(\frac{-2\hat{A}}{c_1}\right)^{0.5} \quad (40)$$

$$R_r = -\frac{k}{c_2}\hat{B}e^{\frac{-k}{c_2}T} \quad (41)$$

Equation (42) can be obtained by substituting ***Equations (37)*** and ***(38)*** into ***Equation (34)***

$$B = X - \frac{F}{k} \quad (42)$$

Considering ***Equation (32)***, the value of parameter x_p (i.e. the displacement of the last point in the compression curve) is obtained as:

$$x_p = Be^{-\frac{k}{c_2}T} + (2\left(\frac{FT-A}{c_1}\right))^{0.5} + \frac{F}{k} \quad (43)$$

The displacement of the first point in the recovery curve is equal to that of the last point in the compression curve as follows:

$$x_p = \hat{B}e^{-\frac{k}{c_2}T} + (-\frac{2\hat{A}}{c_1})^{0.5} \quad (44)$$

The slope of the first point in the compression force can be obtained as:

$$R_{co} = -\frac{k}{c_2}B + \frac{F}{c_1}\left(-\frac{2A}{c_1}\right)^{-0.5} \quad (45)$$

The slope of the last point in the compression curve can be obtained as:

$$R_{cp} = \dot{x} = -\frac{k}{c_2}Be^{-\frac{k}{c_2}T} + \frac{F}{c_1}\left(\left(\frac{FT-A}{c_1}\right)\right)^{-0.5} \quad (46)$$

Considering ***Equation (42)*** and ***(43)*** Constant $\hat{A}$ can be obtained as follows:

$$\hat{A} = -\frac{c_1}{2}(Be^{-\frac{k}{c_2}t} + \frac{F}{k} - \sqrt{\frac{2(F.t-A)}{c_1}} - + \frac{k}{c_2}\hat{B}e^{-\frac{k}{c_2}T} - \hat{B}e^{-\frac{k}{c_2}t})^2 \quad (47)$$

Experimental

In this study, polyester fibres with a fineness of 12 denier and length of 70-90 mm were used to prepare needle-punched non-woven samples. To produce needle–punched nonwoven fabrics with an average mass per unit area of 600 g/m^2 (which is customarily used in industrial applications, such as automotive floor-coverings [1] and geotextiles), 100% polyester fibres were processed on a conventional carding. The fibrous web coming out from the card was then fed to feed a lattice of the horizontal cross-lapper and cross-laid webs produced.

The 8 folded layers were fed to a pair of needle looms, needling from the top and bottom, respectively. Both looms were equipped with Groz-Beckert [14] barbed needles, coded as 15*18*38*3R222G3067 and 15*18*32*3R333G3007. The needling was done at a machine company called "Fehrer". ***Table 1*** shows the needling parameters.

The initial thickness of the sample under a static pressure of (20.2) kpa was measured using a digital thickness tester according to ISO 1765 [15] (with an accuracy of 0.01 mm). Based on the standard method, the sample was cut to 10×10 cm^2 dimensions. Five samples were prepared for each test, and the results were recorded based on the average of the measurements. All the experiments were performed under standard conditions of 222 °C and 652% RH [16].

The thickness reduction of the nonwoven samples was measured under BMSL and PHSL. In order to measure the thickness

Table 1. *Needling parameters.*

Needling stage	Number of strokes, stroke/min	Penetration, mm	Input speed, m/min	Output speed, m/min
Input board, top	520	13.5	2.5	3.4
Output board, bottom	770	9.0	3.4	3.4

__Table 2.__ Thickness reduction of the nonwoven samples under BMSL.

Time, min	Thickness reduction, mm	Time, min	Thickness reduction, mm
0	0.00	70	1.37
10	0.48	80	1.41
20	0.96	90	1.44
30	1.10	100	1.47
40	1.25	110	1.49
50	1.29	120	1.51
60	1.34		

__Table 3.__ Thickness recovery of nonwoven samples after the removal of BMSL.

Time, min	Thickness recovery, mm	Time, min	Thickness recovery, mm
0	1.51	40	1.15
10	1.35	50	1.10
20	1.28	60	1.02
30	1.22		

__Table 4.__ Thickness reduction of nonwoven samples under PHSL.

Time, min	Compression value, mm	Time, min	Compression value, mm	Time, min	Compression value, mm
0	0.00	540	1.69	1080	2.10
60	1.00	600	1.75	1140	2.15
120	1.18	660	1.80	1200	2.19
180	1.29	720	1.85	1260	2.22
240	1.37	780	1.90	1320	2.25
300	1.45	840	1.94	1380	2.26
360	1.51	900	1.99	1440	2.26
420	1.57	960	2.03		
480	1.63	1020	2.07		

__Table 5.__ Thickness recovery of nonwoven samples after the removal of PHSL.

Time, min	Compression value, mm	Time, min	Compression value, mm	Time, min	Compression value, mm
0	2.26	540	1.69	1080	1.53
60	2.03	600	1.66	1140	1.53
120	1.95	660	1.64	1200	1.53
180	1.9	720	1.63	1260	1.52
240	1.85	780	1.61	1320	1.52
300	1.80	840	1.59	1380	1.52
360	1.77	900	1.58	1440	1.52
420	1.74	960	1.57		
480	1.72	1020	1.54		

__Table 6.__ Linear Jeffrey's II model parameters.

Model	c_1, N.s/m	c_2k, s	A, m/s	B, m	$\hat{A}$, m/s	$\hat{B}$, m
Linear Jeffrey's model BMSL	6.864×10^{8}	2.61×10^{3}	-3.2×10^{-7}	-8.3×10^{-4}	-3.93×10^{-6}	8.6×10^{-4}
Linear Jeffrey's model PHSL	1.75×10^{10}	3.09×10^{4}	-3.9×10^{-8}	-1.2×10^{-3}	-4.32×10^{-7}	1.4×10^{-3}

__Table 7.__ Nonlinear Jeffrey's II model parameters.

Model	c_1, N.s/m^2	c_2, N.s/m	k, N/m	A, m/s	B, m	$\hat{A}$, m/s	$\hat{B}$, m
Nonlinear Jeffrey's II model under BMSL	1.36×10^{12}	2×10^{10}	5.1×10^{13}	-4.6×10^{-2}	2.6×10^{-7}	-4.98×10^{5}	1.09×10^{-2}
Nonlinear Jeffrey's II model under PHSL	2.19×10^{13}	1.0×10^{7}	5×10^{16}	-6.99×10^{-8}	-7.99×10^{-11}	-2.56×10^{7}	1.309

reduction rate under BMSL and PHSL, the samples were placed under static loading in accordance with ISO 3415 and ISO3416 [17-18]. A laboratory static loading device was used to simulate the application of the static loading, shown in ***Figure 3***. In this case, the samples were placed under a pressure of 220 kpa for two hours, and the thickness loss was measured every 10 minutes. After the load was removed, the thickness of the samples was measured at 10-minute intervals up to an hour. It should be mentioned that there were five samples to test, and the results were recorded based on the average of the measurements, illustrated in ***Tables 2*** and ***3***.

Figure 4 shows a schematic of the compression value of the nonwoven fabric under static loading. As shown, is the initial thickness, and refers to the thickness of the nonwoven after the compressive force is applied to the sample surface. The displacement is defined as $(x_0 - x_1)$. An increase in the number of impacts led to an increase in the displacement.

In order to measure the thickness reduction rate under PHSL, the samples were placed under static loading in accordance with ISO 3416 [14]. They were subjected to a pressure of 700 kpa for 24 hours, and their thickness was measured during the pressure. After the load was removed, the thickness of the samples was measured up to 24 hours. Five samples were tested, and the results were recorded based on the average of the measurements, illustrated in ***Tables 4*** and ***5***.

Results and discussion

In this study, the compression and recovery properties of needle-punched non-woven textiles were investigated under static loading. Also, the parameters of linear and nonlinear Jeffrey's models under BMSL and PHSL were obtained through analytical processes, listed in ***Tables 6*** and *7*.

Figure 5 shows the experimental data and results obtained from the linear Jeffrey's II model for the compression ***Equation (7)*** and recovery behaviour

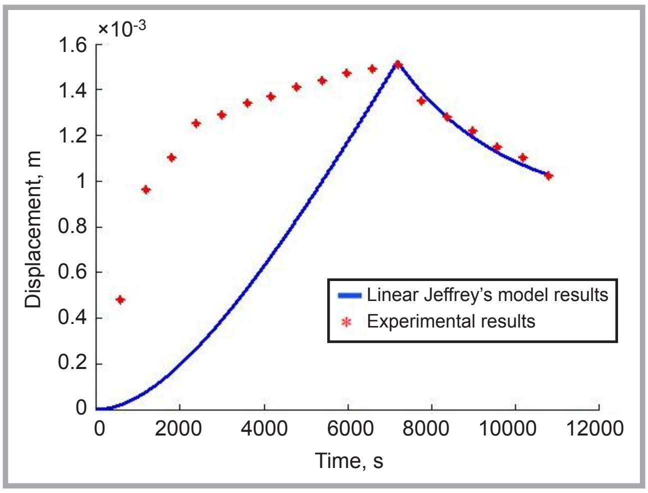

Figure 5. *Comparison of experimental data and results obtained from the linear Jeffrey's model for the compression and recovery behaviour of nonwoven textiles under BMSL.*

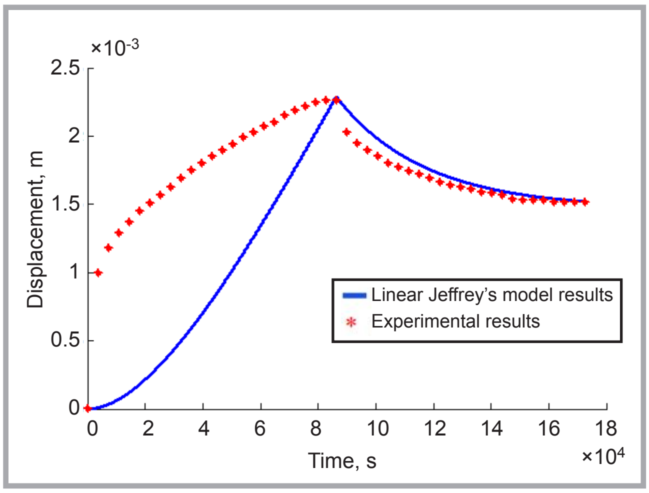

Figure 6. *Comparison of the experimental data and results obtained from the linear Jeffrey's model for the compression and recovery behaviour of nonwoven textiles under PHSL.*

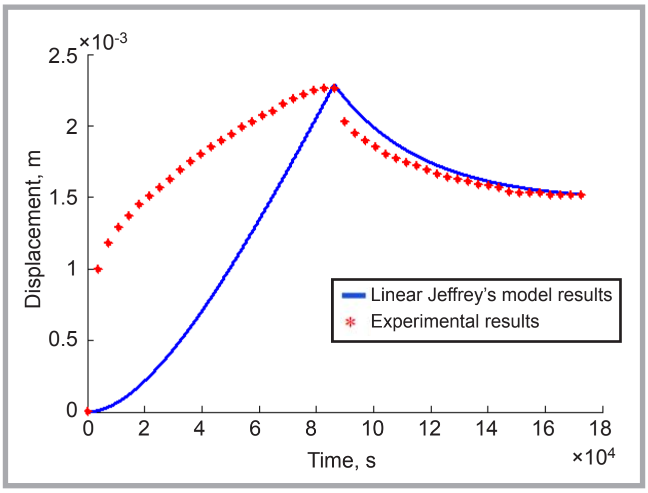

Figure 7. *Comparison of the experimental data and results obtained from the nonlinear Jeffrey's model for the compression and recovery behaviour of nonwoven textiles under BMSL.*

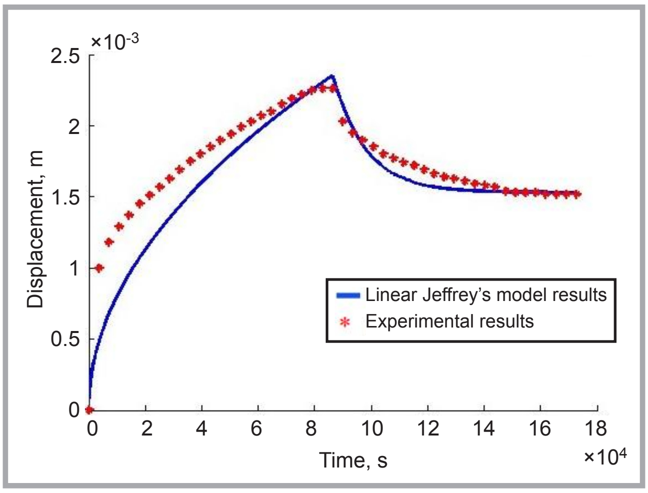

Figure 8. *Comparison of the experimental data and results obtained from the nonlinear Jeffrey's II model for the compression and recovery behaviour of nonwoven textiles under PHSL.*

Equation (12) of the non-woven sample after applying static loading for 120 minutes and an hour after the load removal.

Figure 6 shows the experimental data and results obtained from the linear Jeffrey's model for the compression ***Equation (7)*** and recovery behavior ***Equation (12)*** of the nonwoven sample after applying 24-hour static loading and 24 hours after the load removal.

As can be seen in ***Figures 5*** and ***6***, there is a good correlation between the theory and experimental data for the linear model to predict the recovery behaviour of nonwoven samples under BMSL and PHSL. However, as the results presented in these figures revealed, there is a poor correlation between the theory and experimental data for the linear Jeffrey's model to predict the compression behaviour of nonwoven samples under BMSL and PHSL. In other words, the linear Jeffrey's model is more accurate in predicting the recovery properties under BMSL and PHSL than in predicting the compression properties.

Figures 7 shows the experimental data and results obtained from the nonlinear Jeffrey's model for the compression ***Equation (32)*** and recovery behaviour ***Equation (40)*** of the nonwoven sample after applying 120-min static loading and an hour after the load removal.

Figure 8 shows the experimental data and results obtained from the nonlinear Jeffrey's model for the compression ***Equation (32)*** and recovery behaviour ***Equation (40)*** of the nonwoven sample after applying 24-hour static loading and 24 hours after the load removal.

As can be seen in ***Figures 7*** and ***8***, the nonlinear Jeffrey's II model is capable enough of predicting the compression and recovery behaviour of nonwoven samples under BMSL and PHSL.

Table 8 presents the mean absolute errors obtained from the linear and nonlinear Jeffrey's models under BMSL and PHSL for compression and recovery behaviour.

The results showed that the mean absolute errors were 14.18% and 12.17% for the compression and recovery behaviour in the linear Jeffrey's II model and 4.68% and 4.66% in the nonlinear Jeffrey's II model under BMSL and PHSL, respectively. Thus, the compression and

Table 8. Mean absolute errors for the linear and nonlinear Jeffrey's models

Mechanical model	loading	Compression error value, %	Recovery error value, %	Average error value, %
linear Jeffrey's II model	BMSL	25.34	3.02	14.18
	PHSL	18.48	5.87	12.17
Non-linear Jeffrey's II model	BMSL	7.3	2.07	4.68
	PHSL	5.96	3.37	4.66

Table 9. Comparison of methods developed by researchers

Year	Authors	Product	Mechanical behaviour	loading	Loading	Comparison method of experimental and theoretical results
2016	Jafari and Ghane	Carpet	Recovery	Linear	BHSL	Fitting
2017	Khavari and Ghane	Carpet	Compression and Recovery	Linear and non-linear	BHSL	Fitting
2018	Jafari and Ghane	Carpet	Recovery	Linear and non-linear	BHSL	Fitting
2020	Presented study	Nonwoven	Compression and Recovery	Linear and non-linear	BMSL and PHSL	Analytical solution

recovery behaviour can be predicted in the nonlinear Jeffrey's II models under BMSL and PHSL better than in the linear Jeffrey's II model.

In the prediction of the compression and recovery behavior for the nonlinear Jeffrey's II model under BMSL and PHSL; the mean absolute errors were 7.3%, 2.07%, 5.96% and 3.37%, respectively.

In the prediction of the recovery behaviour for the linear Jeffrey's II model under BMSL and PHSL the mean absolute errors were 3.02% and 5.87%, respectively. The magnitude of compression errors in the linear Jeffrey's II model under BMSL and PHSL were significant, which can be due to the extreme deformation of the samples at the start of the loading and the lack of ability of the model recommended to predict this change at the same speed.

Table 9 shows a comparison of various investigations with the methods developed in this study with respect to simulation of the compression and recovery behaviour of textiles.

Conclusions

In this study, two different mechanical models based on mass-spring-dashpot including linear and nonlinear Jeffrey's II models were developed to predict the compression and recovery behaviour of needle-punched non-woven textiles for automotive floor-covering application under brief, moderate static loading (BMSL) and prolonged, heavy static loading (PHSL) according to ISO 3415 and ISO 3416, respectively. Through solving the governing equation of the model to obtain the model parameters analytically, thickness loss of the nonwoven textiles within a certain time was achieved. The results obtained from the two models were compared with experimental results in four cases including the linear and nonlinear Jeffrey's II model under BMSL and PHSL. It was shown that the nonlinear Jeffrey's model is sufficiently able to predict the compression and recovery behaviour of nonwoven textiles under BMSL and PHSL. However, the linear Jeffrey's II model can predict recovery properties under BMSL and PHSL more accurately than compression properties.

References

1. Atakan R, Sezer S, Karakas H. Development of Nonwoven Automotive Carpets Made of Recycled PET Fibers with Improved Abrasion Resistance. *J Ind Text*. 2018; 48: 1-23.
2. Kothari VK, Das A. Time-Dependent Behavior of Compression Properties of Nonwoven Fabrics. *Indain J Fibre Text Res*. 1994; 19: 58-60.
3. Kothari VK, Das A. An Approach to the Theory of Compression of Nonwoven Fabrics. *Indain J Fibre Text Res*. 1996; 21: 235-243.
4. Debnath S, Madhusoothanan M. Modeling of Compression Properties of Needle-punched Nonwoven Fabrics Using Artificial Neural Nwtwork *2008;* 33: 392-399.
5. Debnath S, Madhusoothanan M. Compression Properties of Polyester Needle-Punched Fabric. *J Eng Fibers Fabr 2009;* 4: 14-19.
6. Debnath S, Madhusoothanan M. Studies on Compression Properties of Polyester Needle-punched Nonwoven Fabrics under Dry and Wet Conditions. *J Ind Text* 2011; 41: 292-308.
7. Debnath S, Madhusoothanan M. Studies on Compression Properties of Polyester Needle-punched Nonwoven Fabrics under Wet Conditions. *Fiber Polym* 2013; 14(5): 854-859.
8. Jafari S, Ghane M. An Analytical Approach for the Recovery Behavior of Cut Pile Carpet after Static Loading by Mechanical Models. *Fiber Polym 2016;* 17: 651-655.
9. Khavari S, Ghane M. Aanalytical Approach for the Compression and Recovery Behavior of Cut Pile Carpets under Constant Rate of Compression by Mechanical Models. *Fiber Polym 2017;* 18: 190-195.
10. Tower TT, Carrillo A. *Science in the Age Experience 2017; may 15-18, Chicago:* 296-305.
11. Jafari S, Ghane M. Analysis of the Effect of UV Radiation on the Recovery Properties of Pile Carpet after Static Loading through Analytical and Viscoelastic Modeling. *J Text I* 2017; 108: 1905-1909.
12. Jafari S, Ghane M. Viscoelastic Modeling of the Recovery Behavior of Cut Pile Carpet after Static Loading: A Comparison between Linear and Nonlinear Models. *J Text Poly* 2018; 6(1): 9-14.
13. Daniel D. Joseph *.Fluid Dynamics of Viscoelastic Liquids.*1st edition, 1990.
14. Groz-Beckert. Needles; general catalogue. Germany: Groz-Beckert, 2009.
15. International Standard. ISO 1765. Machine Made Textile Floor Coverings-Determination of Thickness. 1986.
16. ISO 139:2005. Textiles-Standard Atmospheres for Conditioning and Testing.
17. International Standard. ISO 3415. Textile Floor Covering – Determination of Thickness Loss After Brief, Moderate Static Loading. 1986.
18. International Standard. ISO 3416. Textile Floor Covering – Determination of Thickness Loss After Polonged, Heavy Static Loading. 1986.

Received 30.06.2020 Reviewed 08.01.2021